

Article

SO₄²⁻/Sn-MMT Solid Acid Catalyst for Xylose and Xylan Conversion into Furfural in the Biphasic System

Qixuan Lin ¹, Huiling Li ², Xiaohui Wang ¹, Longfei Jian ¹, Junli Ren ^{1,*}, Chuanfu Liu ¹ and Runcang Sun ³

¹ State Key Laboratory of Pulp and Paper Engineering, South China University of Technology, Guangzhou 510640, China; linqixuan7@163.com (Q.L.); wxhui006@163.com (X.W.); johnnycruise69@gmail.com (L.J.); chfliu@scut.edu.cn (C.L.)

² Guangdong Key Laboratory for Innovative Development and Utilization of Forest Plant Germplasm, State Key Laboratory for Conservation and Utilization of Subtropical Agro-Bioresources, South China Agricultural University, Guangzhou 510642, China; lihl@scau.edu.cn

³ Beijing Key Laboratory of Lignocellulosic Chemistry, College of Materials Science and Technology, Beijing Forestry University, Beijing 100083, China; rcsun3@bjfu.edu.cn

* Correspondence: renjunli@scut.edu.cn; Tel./Fax: +86-20-8711-1861

Academic Editors: Shaobin Wang and Xiaoguang Duan

Received: 22 February 2017; Accepted: 11 April 2017; Published: 17 April 2017

Abstract: A sulphated tin ion-exchanged montmorillonite (SO₄²⁻/Sn-MMT) was successfully prepared by the ion exchange method of montmorillonite (MMT) with SnCl₄, followed by the sulphation. This catalysis was applied as a solid acid catalyst for the heterogeneous catalytic transformations of xylose and xylan into furfural in the bio-based 2-methyltetrahydrofuran/H₂O biphasic system. These prepared catalysts were characterized by X-ray powder diffraction (XRD), Fourier transform infrared spectroscopy (FTIR), temperature programmed desorption of ammonia (NH₃-TPD), pyridine adsorbed Fourier transform infrared spectroscopy (Py-FTIR), element analysis (EA) and Brunauer-Emmett-Teller (BET) method. Their catalytic performance for xylose and xylan into furfural was also investigated. The reaction parameters such as the initial xylose and xylan concentration, the amounts of catalyst, the organic-to-aqueous phase volume ratio, the reaction temperature and time were studied to optimize the reaction conditions. Results displayed that SO₄²⁻/Sn-MMT contained both Brønsted acid and Lewis acid sites, and SO₄²⁻ ions were contributive to the formation of stronger Brønsted acid sites, which could improve the reaction efficiency. Reaction parameters had significant influence on the furfural production. The substitution of water by the saturated NaCl solution in the aqueous phase also had an important effect on the xylose and xylan conversion. The highest furfural yields were achieved up to 79.64% from xylose and 77.35% from xylan under the optimized reaction conditions (160 °C, 120 min; 160 °C, 90 min). Moreover, the prepared catalyst was stable and was reused five times with a slight decrease (10.0%) of the furfural yield.

Keywords: solid acid catalyst; xylan; xylose; conversion; furfural; biphasic system

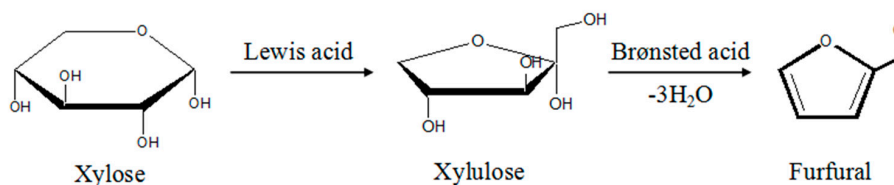
1. Introduction

With the rapid development of industrialization in the world, toxic pollutant in water remains a great concern to the environment. Especially in many chemical reactions, the conventional homogeneous catalyst, such as mineral acids, could produce a large amount of acid wastewater, which is toxic and corrosive in nature. Moreover, the homogeneous catalyst can also lead to an extra neutralization step, a tedious purification process and an increase of production cost. Thus, the heterogeneous catalyst, which generally appears in solid form, acts in a dissimilar phase in the liquid reaction mixture [1],

and is strongly desired to be developed due to its outstanding advantages such as environmental benefits, reusability, efficient conversion, easy separation and purification of the product [2].

The heterogeneous catalyst was widely applied in the production of furfural, which is a renewable bio-based chemical derived from the pentosan-rich lignocellulosic biomass with an annual production capacity of more than 200,000 tons [3], and which can be advantageous in many fields, such as oil refining, plastics and agrochemical industries. Solid acid catalysts, such as functionalized partially hydroxylated MgF_2 [4], SBA-15- SO_3H [5] and silica-poly (styrene sulphonic acid) [6] with micro/mesoporous, are highly effective in the furfural production.

It has been proposed that the conversion of xylose to furfural involves two steps: the first isomerization of xylose to xylulose using Lewis acid catalysts, and then followed by the dehydration of xylulose to furfural catalyzed by Brønsted acid (Scheme 1) [7,8]. Metal cations such as Sn^{4+} , Cr^{3+} , Al^{3+} acting as Lewis acids were beneficial for the conversion of xylose to xylulose, and our group found that SnCl_4 was the most effective catalyst for the furfural production, compared with other metal chlorides [9]. However, the chromium ion is toxic and these homogeneous catalysts are unable to recycle, thus a desirable heterogeneous catalyst containing Sn^{4+} need to be designed. Montmorillonite (MMT) is composed of regular layers, and holds exchangeable cationic species, which are easy to be substituted by metal cations and designated as X-MMT (X = metal). Sn-MMT was widely used in many organic reactions [10,11], and our previous study found that Sn-MMT rapidly prepared under microwave irradiation demonstrated the excellent catalytic performance in the conversion of xylose, water-insoluble hemicelluloses and water-soluble fraction of corncob. In that study, a 76.79% furfural yield was directly obtained from xylose in a new biphasic system with 2-s-butylphenol (SBP) as the organic extracting layer and dimethyl sulfoxide (DMSO) as the co-solvent in contact with an aqueous phase saturated with NaCl (SBP/NaCl-DMSO) [12]. Additionally, it was found that the acidity of a solid catalyst can be modified by the treatment with sulfuric acid to form the solid super acid catalyst, because the SO_4^{2-} ions can intensely draw the electrons around the metal ions to lead to the formation of strong Brønsted acid sites [13], promoting the catalyst activity.



Scheme 1. Two steps of the conversion of xylose to furfural.

To improve the furfural yield in a green way, different solvent systems have been developed. Monophasic systems such as dimethyl sulfoxide (DMSO) [14], tetrahydrofuran (THF) [15], 1-butanol [16], and ionic liquids [17] have been investigated for the furfural preparation. Biphasic systems consisting of water and the organic solvent are more efficient, in which furfural produced in the aqueous phase can be immediately extracted into the organic phase. Thus the undesired side reaction between furfural and intermediate or other compounds could be suppressed [18]. The commercially available solvent 2-Methyltetrahydrofuran (2-MTHF) is derived based on lignocellulose. It is only partially miscible with water, and the separation temperature at 60 °C is desirable because the solubility of 2-MTHF in water drops from 14.5% at 20 °C to 6.6% at 60 °C [19]. It is also stable in acid or base conditions with other excellent advantages such as low toxicity, easy recycling and environmentally friendly features [9].

To further improve the catalytic performance of Sn-MMT and enhance the furfural yield in a green way, SO_4^{2-} ions were loaded on Sn-MMT by the impregnation method and 2-MTHF was used as the organic solvent for the furfural production from xylose and xylan in this work, aiming to reduce the amount of catalyst used and to achieve high furfural yields at more moderate conditions in the green catalytic process. The prepared catalyst was characterized by X-ray powder diffraction (XRD),

Fourier transform infrared spectroscopy (FTIR), temperature programmed desorption of ammonia (NH_3 -TPD), pyridine adsorbed Fourier transform infrared spectroscopy (Py-FTIR), element analysis (EA) and Brunauer-Emmett-Teller (BET) method. This solid acid catalyst was also employed for the transformation of xylose and xylan into furfural in the biphasic system with 2-MTHF as the organic solvent. Furthermore, the reaction parameters such as the initial xylose and xylan concentration, the amounts of catalyst, the volume ratio of the organic phase and the aqueous phase, the reaction temperature and time were investigated to optimize the reaction conditions. The reusability of this catalyst was also discussed.

2. Results and Discussion

2.1. Characterization of Catalyst

MMT is able to intercalate various ions into the interlayer spaces, which would influence the interlayer distance [20]. The 001 reflection of the XRD patterns showed the basal spacing of MMT (Figure 1). The ‘ d_{001} ’ values of MMT and Sn-MMT were 14.76 Å and 14.93 Å, respectively, which confirmed that the structure of MMT was still maintained and the ion-exchanging process had no influence on the structure of the MMT material [21]. On the other hand, the ‘ d_{001} ’ value of SO_4^{2-} /Sn-MMT increased to 17.13 Å, indicating that the intercalation of SO_4^{2-} ions into the layered Sn-MMT, and the multilayered regularity of Sn-MMT, might be slightly damaged during the impregnation due to the high polarizability of SO_4^{2-} ions. The sharp peak at $2\theta = 27.94^\circ$ of MMT was broadened in Sn-MMT and SO_4^{2-} /Sn-MMT due to the formation of $\text{Sn}(\text{OH})_4$ species [22]. It was reported that partially hydrolyzed Sn-OH groups acted as Brønsted acid and Sn^{4+} ions acted as Lewis acid for the glucose conversion [21], which implied that SO_4^{2-} /Sn-MMT contained both Brønsted acid and Lewis acid sites, and the role of SO_4^{2-} ions could be intensely drawing the electrons around the Sn^{4+} ions of Sn-OH groups to form stronger Brønsted acid sites, consequently leading to improvement in the reaction efficiency [13].

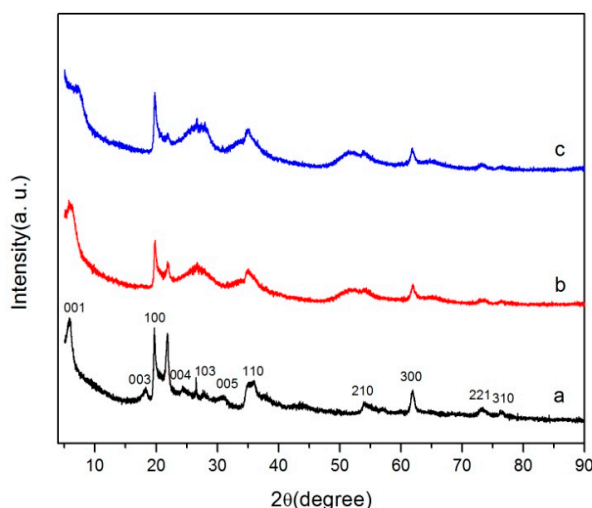


Figure 1. XRD patterns of (a) montmorillonite (MMT); (b) Sn-MMT; (c) SO_4^{2-} /Sn-MMT.

The wave number and assignment of the main vibration modes in the FTIR spectra of MMT, Sn-MMT and SO_4^{2-} /Sn-MMT (Figure 2) were obtained (Table 1) based on a previous report [23]. The FTIR spectrum of Sn-MMT was nearly identical in the FTIR skeleton of MMT, because the ion-exchanging process had no influence on the structure of the MMT material. Compared with MMT and Sn-MMT, the characteristic bands at ~ 3630 , 1104, 909, 835, 619, 519, 461 cm^{-1} in the FTIR spectrum of SO_4^{2-} /Sn-MMT were distinctly weakened, which was attributed to the break of the multilayered and regular structure of clay. This result was well supported by the XRD analysis. The water can be

polarized by exchanged cations in the interlayer space of MMT, and the vibration bands centered at ~ 3429 and 1637 cm^{-1} were attributed to the stretching and bending vibrations of adsorbed water, respectively. The reduction at ~ 3429 and 1637 cm^{-1} in the FTIR spectra of $\text{SO}_4^{2-}/\text{Sn-MMT}$ implied the loss of interlayer water, which indirectly proved the destruction of the MMT structure.

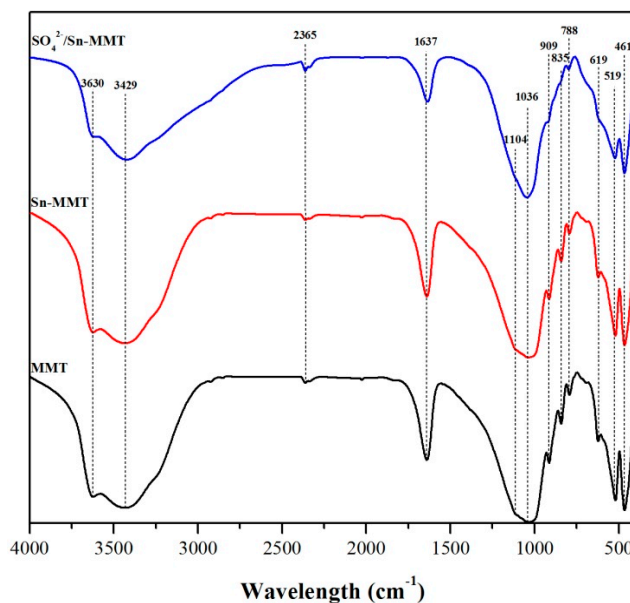


Figure 2. FTIR spectra of MMT, Sn-MMT and $\text{SO}_4^{2-}/\text{Sn-MMT}$.

Table 1. Position and assignment of the FTIR vibration bands.

Position (cm^{-1})	Assignment
3630	Structural Al–OH stretching
3429	H–OH stretching of adsorbed water
2365	O=C=O stretching
1637	H–OH bending of adsorbed water
1104	Si–O stretching
1036	Si–O–Si stretching
909	Al–OH bending
835	Al–Mg–OH deformation
788	Si–O stretching of quartz
619	Coupled Al–O and Si–O out-of-plane
519	Al–O–Si deformation
461	Si–O–Si deformation

The acid properties of this catalyst were examined by NH_3 -TPD (Figure 3). In the NH_3 -TPD curves of the catalyst, peaks are generally observed in five temperature regions. The peaks appearing at $\leq 150\text{ }^\circ\text{C}$ corresponded to the physically adsorbed and hydrogen-bound NH_3 [24,25], and the regions at $150\text{--}250\text{ }^\circ\text{C}$, $250\text{--}350\text{ }^\circ\text{C}$, $350\text{--}500\text{ }^\circ\text{C}$, and $>500\text{ }^\circ\text{C}$ were defined as weak, medium, strong and very strong acid sites, respectively. The stronger acid sites corresponded to a higher desorption temperature of NH_3 adsorbed on the acid sites [26], thus weak acid sites existed in $\text{SO}_4^{2-}/\text{Sn-MMT}$ and Sn-MMT. NH_3 -TPD revealed that total acidity of $\text{SO}_4^{2-}/\text{Sn-MMT}$ and Sn-MMT catalysts were 0.58 and 0.35 mmol of NH_3 desorbed g^{-1} .

Py-FTIR is a powerful surface analytical technique for discernment of Brønsted and Lewis acid sites. The adsorbed pyridine probe molecules tend to couple with aprotic (Lewis) and/or protonic (Brønsted) catalytic centers through the nitrogen lone-pair electrons to form coordinative bonded pyridine complexes and/or pyridium ions, and hence can be detected by monitoring their ring vibrations [27]. Figure 4 illustrates Py-FTIR spectra of Sn-MMT and $\text{SO}_4^{2-}/\text{Sn-MMT}$, in which these characteristic

bands are in the range of $1400\text{--}1700\text{ cm}^{-1}$. The coexistence of Brønsted acid sites (at 1542 and 1636 cm^{-1}) and Lewis acid sites (at 1453 and 1614 cm^{-1}) are evident for $\text{SO}_4^{2-}/\text{Sn-MMT}$ catalyst. In addition, another peak at about 1489 cm^{-1} was characteristic of pyridine adsorbed on both Lewis and Brønsted acid sites. A minor peak at 1542 cm^{-1} (B) and the disappeared peak at 1636 cm^{-1} (B) of Sn-MMT indicated that small amount of Brønsted acid sites existed on Sn-MMT. The intensity of all peaks was increased after loading of SO_4^{2-} ions, implying the stronger acid site of $\text{SO}_4^{2-}/\text{Sn-MMT}$ catalyst.

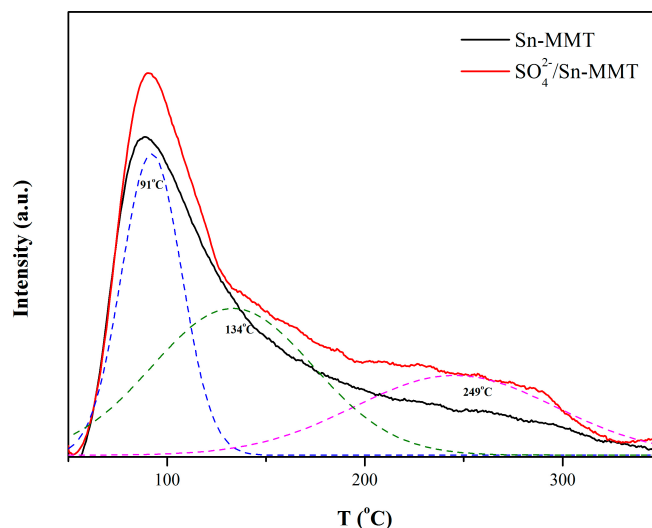


Figure 3. Temperature programmed desorption of ammonia (NH_3 -TPD) profile of the $\text{SO}_4^{2-}/\text{Sn-MMT}$ and Sn-MMT catalysts.

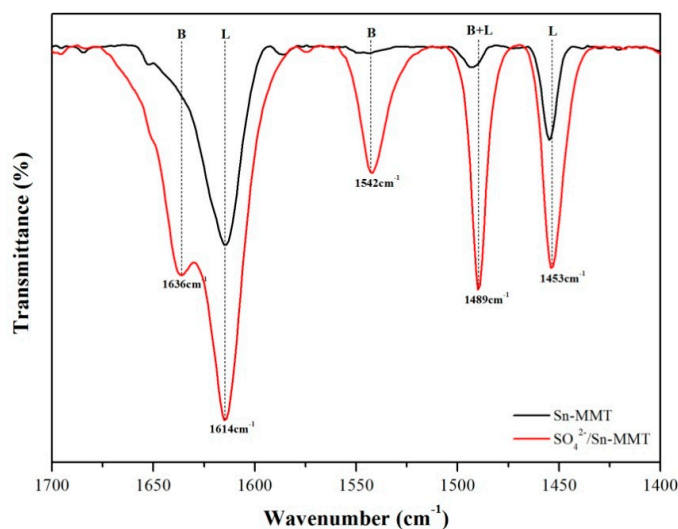


Figure 4. Pyridine-adsorbed FTIR spectra on Sn-MMT and $\text{SO}_4^{2-}/\text{Sn-MMT}$.

Elemental analysis by inductively coupled plasma (ICP) (Table 2) showed that the content of Sn in Sn-MMT was 15.32 wt %, indicating that tin ions were successfully intercalated into the MMT framework by replacing calcium and sodium ions. Additionally, the S content of $\text{SO}_4^{2-}/\text{Sn-MMT}$ increased promptly, suggesting that the successful introduction of SO_4^{2-} ions on the catalyst. The nitrogen sorption data showed that the BET surface area greatly increased from $42.38\text{ m}^2\text{ g}^{-1}$ of MMT to $178.94\text{ m}^2\text{ g}^{-1}$ of Sn-MMT with a porous structure. Moreover, the BET surface area, micropore volume and pore diameter of $\text{SO}_4^{2-}/\text{Sn-MMT}$ had a slight decrease, due to loading of SO_4^{2-} groups on the surface of pore channels, causing the slight structural destruction and collapse [28].

Table 2. Properties of catalysts.

Samples	Elemental Content (wt %)				BET Surface Area (m ² g ⁻¹)	Micropore Volume (cm ³ g ⁻¹)	Pore Diameter (nm)
	Ca	Na	Sn	S			
MMT	3.44	0.54	-	-	42.38	0.18	9.15
Sn-MMT	0.94	0.16	15.32	-	178.94	0.27	12.37
SO ₄ ²⁻ /Sn-MMT	0.65	0.12	11.20	2.79	153.52	0.10	8.61

2.2. Furfural Production from Xylose and Xylan

2.2.1. Effect of Substrate Concentration

Substrate concentration had a significant influence on the furfural yield for heterogeneous catalytic reactions. Figure 5a shows the effect of initial xylose and xylan concentrations including 5 g/L to 100 g/L on the conversion of xylose and xylan to furfural. The furfural yields first increased and then decreased for xylose conversion. When the xylose concentration was 20 g/L, the highest furfural yield was achieved up to 45.36%. When the xylose concentration was above 20 g/L, the furfural yields were decreased, which were 44.21%, 40.27%, 38.64%, 33.14% and 32.98%, respectively, correspondingly at the xylose concentration of 25, 30, 35, 40 and 45 g/L. The similar trend occurred for the xylan conversion. The highest furfural yield was 42.34% at the xylan concentration of 10 g/L. The further increase of the initial substrate concentration had a negative influence on the furfural yield. When the substrate concentration was increased to 100 g/L, the furfural yields of xylose and xylan declined to 27.81% and 23.61%, respectively. The partial loss of furfural might be attributed to the higher substrate concentration leading to higher rates of side reactions such as the reaction of xylose and furfural to form humins [9,29]. The desirable initial xylose and xylan concentrations were kept at 20 g/L and 10 g/L, respectively.

2.2.2. Effect of the Catalyst Amount

The catalyst amount ranging from 0.05 to 1.5 g/g substrate was investigated in this case (Figure 5b). The furfural yield first increased for both xylose and xylan. The maximum furfural yields were achieved up to 44.95% from xylose and 46.58% from xylan when the amounts of catalyst were 0.5 g/g substrate and 1.0 g/g substrate, respectively. After the optimal catalyst amount, there was an obvious decline for furfural yield. The reaction took place on the surface of the catalyst where the acid sites existed and the acid sites were proportional to the amount of catalyst [13]. When excessive catalyst was added, superfluous active sites led to the occurrence of side reactions [30]. The optimum amounts of catalyst were 0.5 g/g substrate for xylose and 1.0 g/g substrate for xylan, respectively.

2.2.3. Effect of the 2-MTHF/Water Volume Ratio

The formation of furfural occurs in the aqueous phase, and the organic solvent can immediately extract furfural into organic phase, inhibiting the undesired side reaction. A stable solvent, 2-MTHF can be derived from renewable resources has a low miscibility with water and a high extraction ability for furfural [9]. As shown in Figure 5c, comparing the volume ratio of 0 with the volume ratio of 2:5, the addition of 2-MTHF markedly improved the furfural yield. Subsequently, with the increase of the 2-MTHF/water volume ratio from 2:5 to 4:5, furfural yield steadily increased. However, further increasing the ratio, the decrease in furfural yield occurred, which was due to the decrease in extracting power of solvent [31]. Therefore, the appropriate volume ratio needs to be determined, and a ratio of 4:5 was required in this biphasic system for both xylose and xylan. Moreover, the furfural yield from xylan was entirely higher than xylose in Figure 3, which was possibly attributed to the gradual release of xylose from the xylan chain, reducing the side reaction of xylose with furfural.

2.2.4. Effect of Saturated NaCl Solution in the Aqueous Phase

The addition of NaCl in the aqueous phase of the biphasic systems could improve the furfural formation rate in some catalytic systems [12,32] because of its effective separation and the improvement of extracting efficiency of the organic layer [33]. Thus, the saturated NaCl aqueous solution substituted for water phase in the biphasic system was investigated (Figure 5d). The furfural yields of xylose and xylan in the 2-MTHF/water system were 67.02% (10.47%/56.55%, aqueous (A)/organic (O) phase) and 75.71% (15.06%/60.65%, A/O), respectively. For xylose, there was a 12.62% (2.62%/77.02%, A/O) increase when replaced H₂O with saturated NaCl solution, revealing that the addition of NaCl can greatly improve the partitioning of furfural into the organic phase. This result was consistent with the reported in literatures [12,32]. On the other hand, the furfural yield of xylan in the saturated NaCl medium decreased to 62.28% (1.04%/61.24%, A/O), which may be attributed to the high concentration of Cl⁻ ions. Cl⁻ ions acted as catalysts in the enolization reaction of xylose and thus favoring the subsequent dehydration reactions of xylose to furfural [34]. In the absence of NaCl, the catalytic performance of SO₄²⁻/Sn-MMT at different reaction times was also studied (Figure S1). It was demonstrated that in the absence of NaCl, the furfural yield was close to 70% at a long reaction time, proving that the addition of NaCl made the reaction system more efficient.

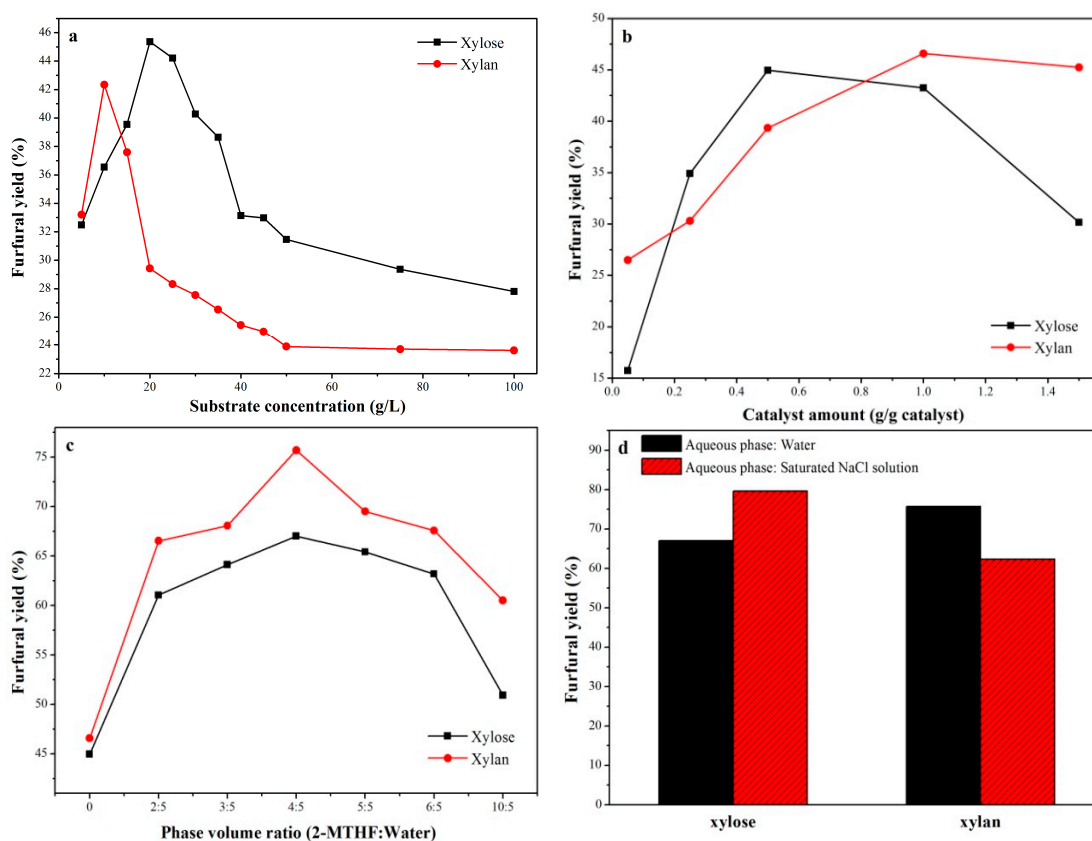


Figure 5. Effects of different reaction parameters on the furfural yield. Reaction conditions: All samples reacted in a hydrothermal reactor at 160 °C for 2 h. (a) 0.5 g/g substrate of catalyst; (b) 20 g/L of xylose, 10 g/L of xylan; (c) 20 g/L of xylose, 0.5 g/g substrate of catalyst; 10 g/L of xylan, 1.0 g/g substrate of catalyst; (d) 20 g/L of xylose, 0.5 g/g substrate of catalyst, volume ratio (organic:aqueous) = 4:5; 10 g/L of xylan, 1.0 g/g substrate of catalyst, volume ratio (organic:aqueous) = 4:5.

2.2.5. Effect of Reaction Temperature and Time

The effect of temperature and time on the transformation of xylose and xylan into furfural in the biphasic system using SO₄²⁻/Sn-MMT as catalysts was studied by conducting the experiments at

different temperatures (150, 160 and 170 °C) in a time range of 30–150 min in Figure 6. For Figure 6a,d, when prolonging the reaction time, the curves of furfural yields had similar appearances: initially increasing to the highest value and then decreasing. The reason of the curves slump was due to the formation of soluble degradation products and black insoluble solids [12]. At lower temperature (150 °C), the lower reaction rate caused the incomplete conversion of xylose to furfural. At higher temperature (170 °C), the side reaction is the major factor leading the reduction of furfural yield [35,36]. The highest furfural yield of xylose and xylan under the investigated conditions were 79.64% at 160 °C for 120 min and 77.35% at 160 °C for 90 min. Figure 6c shows that the furfural selectivity had the similar trend with the furfural yield and the highest furfural selectivity was 80.84% at 160 °C for 120 min. However, the increased temperature and time led to the high consumption rate of xylose and the xylose conversion was increased firstly and then flattened out (Figure 6b). With prolonging the reaction time, the xylose conversion increased from 78.90% at 150 °C for 30 min to 98.73% at 150 °C for 150 min. Moreover, high temperature also led to the high xylose conversion. For example, when the reaction time reached 60 min, the xylose conversion of 98.42% at 170 °C was higher than samples at 160 °C (92.54%) and 150 °C (84.54%). For the reactor time of 150 min, all the samples reacted almost completely. Consequently, the tougher reaction conditions led to the higher xylose conversion. Compared with the Sn-MMT catalyst at the same reaction condition (Supplementary Materials), the furfural yield was increased when SO_4^{2-} /Sn-MMT was used as the catalyst (79.64% vs. 61.22%), which indicated that SO_4^{2-} loading on Sn-MMT significantly improved the catalytic efficiency.

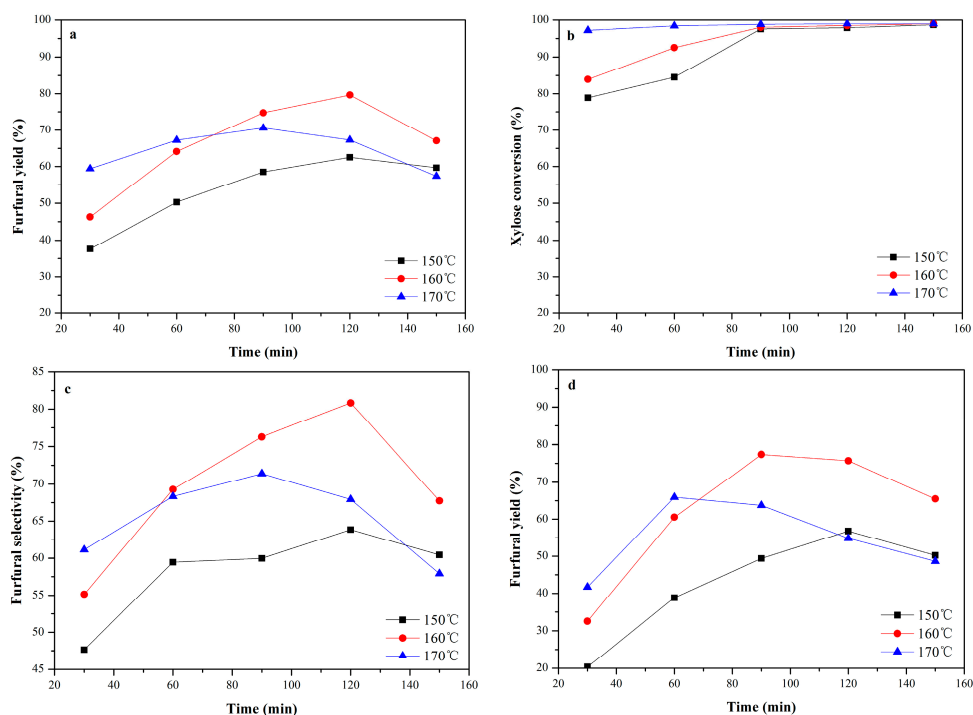


Figure 6. Effects of the reaction temperature and time on the furfural production. Reaction conditions: (a–c) 20 g/L of xylose, 0.5 g/g substrate of catalyst, $V_{2\text{-MTHF}}/V_{\text{NaCl}} = 4:5$; (d) 10 g/L of xylan, 1.0 g/g substrate of catalyst, $V_{2\text{-MTHF}}/V_{\text{water}} = 4:5$.

Table 3 displays the comparison of different procedures for the furfural production. In general, high furfural yields could be easily achieved using mineral acids as catalyst such as sulfuric acid [37]), but it is toxic and corrosive. Other homogeneous catalysts containing Lewis acid such as CrCl_2 and LiBr [38] gave a furfural yield about 60%, but there were disadvantages of homogeneous catalysts, such as the difficulty of separation and recycle, and these limitations provoked the focus on heterogeneous catalysts because they are recyclable and environmentally friendly. Lessard et al. [39]

got a 98% furfural yield, but the required temperature was really high (260 °C). Agirrezabal et al. [40] and Bhaumik et al. [41] also achieved a high furfural yield (more than 80%) but it required a long reaction time. The reaction conditions used in this work were relatively moderate with the furfural yield of 79.64% from xylose and 77.35% from xylan.

Table 3. The comparison of different procedures for the furfural production.

No.	Substrate	Catalyst	Solvent	Temperature	Time	Yield	Refs.
1	Xylose	CrCl ₂ , LiBr	<i>N,N</i> -dimethylacetamide	100 °C	4 h	56%	[38]
2	Xylose	MCM-41-SO ₃ H	toluene/water	140 °C	24 h	75.5%	[42]
3	Xylose	PSZ-MCM-41	toluene/water	160 °C	4 h	42.8%	[43]
4	Xylose	Dealumin. HNu-6 (2)	toluene/water	170 °C	4 h	47%	[44]
5	Xylose	H-mordenite 13	toluene/water	260 °C	0.05 h	98%	[39]
6	Xylose	Arenesulfonic SBA-15	toluene/water	160 °C	20 h	86%	[40]
7	Hydrolysates from corncob	Tin-loaded montmorillonite	SBP/NaCl-DMSO	190 °C	10 min	57.80%	[45]
8	Isolated hemicellulose	Silicoaluminophosphate	toluene/water	170 °C	10 h	82%	[41]
9	Bagasse	Silicoaluminophosphate	toluene/water	170 °C	8 h	93%	[41]
10	Maple wood	Sulfuric acid	methyl isobutyl ketone/water	170 °C	50 min	85.3%	[37]
11	Xylose	SO ₄ ²⁻ /Sn-MMT	2-MTHF/water-NaCl	160 °C	2 h	79.64%	In this work
12	Xylan	SO ₄ ²⁻ /Sn-MMT	2-MTHF/water	160 °C	1.5 h	77.35%	In this work

2.3. Catalyst Recyclability

Catalyst stability is an important factor that could affect the overall reaction process. Thus, the catalyst prepared in this work was recycled five times to study the recyclability under the optimized reaction conditions in Figure 7. After each cycle, catalyst was washed with ethanol and distilled water, dried at 105 °C and reused. In comparison to the catalytic performance of the fresh catalyst, the furfural yields were decreased by 1.5%–10.0% after the one to five recycles, which indicated that the catalytic performance decreased to a slight extent after the fifth regeneration and this catalyst had the excellent reusability. The element analysis of used catalysts (Table S1) showed that after five recycles, the contents of sulfur and tin had a very slight reduction, which meant that the activity of SO₄²⁻/Sn-MMT still remained efficient.

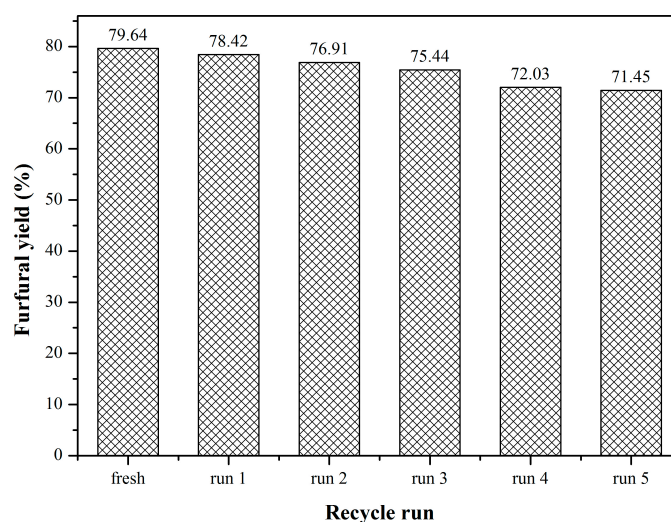


Figure 7. Catalyst recycles experiment. Reaction conditions: 20 g/L of xylose, 0.5 g/g substrate of catalyst, $V_{2\text{-MTHF}}/V_{\text{NaCl}} = 4:5$, 160 °C, 120 min.

3. Materials and Methods

3.1. Materials

Beechwood xylan (AR, $\geq 90\%$) and standard reagents such as D-xylose and furfural were provided by Sigma-Aldrich (Saint Louis, MO, USA). $\text{SnCl}_4 \cdot 5\text{H}_2\text{O}$ (AR, $\geq 99.0\%$) was purchased from Lingfeng Chemical Regent Co., Ltd. (Shanghai, China). MMT (GR, 98%) was obtained from Chengdu Gracia Chemical Technology Co., Ltd., (Chengdu, China). The 2-MTHF (AR, $\geq 99.5\%$), H_2SO_4 (AR, 98%) and NaCl (AR, 99.5%) were supplied by Tianjin Kermel Chemical Regent Co., Ltd., (Tianjin, China). All reagents were used without any purification.

3.2. Preparation of the Catalyst

The Sn-MMT was synthesized according to the methods described in literature [12] with slight modifications. Four grams of MMT was dispersed in ultrapure water (196 mL) and intensely stirred for 30 min at room temperature, followed by standing for 24 h to make it fully swell. Then aq. $\text{SnCl}_4 \cdot 5\text{H}_2\text{O}$ (6.8 mmol, 20 mL) was added slowly. The mixture was treated at 85 °C for 2 h under microwave irradiation (600 W, XH-300UL, Beijing Xiang-Hu Science and Technology Development Reagent Co., Ltd., Beijing, China) at atmospheric pressure. The collected clay was washed with ultrapure water till a neutral pH value was achieved and then the clay was dried at 110 °C over night to form Sn-MMT. Then Sn-MMT was impregnated with 1.0 M H_2SO_4 at the proportion of 20 mL/g for 6 h, then filtrated and oven-dried at 105 °C for 12 h and milled to get the targeted catalyst $\text{SO}_4^{2-}/\text{Sn-MMT}$.

3.3. Characterization of Catalyst

XRD patterns of samples were recorded on a Bruker D8 ADVANCE X-ray diffractometer with $\text{Cu K}\alpha$ radiation (Bruker Corporation, Karlsruhe, Germany). The tube voltage was 40 Kv and the current was 40 mA. The selected 2θ range was 5°–90°, scanning at a step of 0.02°. The Fourier transform infrared (FTIR) spectra were recorded on a spectrophotometer (Tensor 27, Bruker Corporation, Karlsruhe, Germany).

The TPD analysis was performed using a TP 5000-II multiple adsorption apparatus (Tianjin Xianquan Corporation of Scientific Instruments, Tianjin, China). Approximately 100 mg of catalyst was pretreated in a nitrogen atmosphere at 150 °C for 30 min. When the mass baseline was stable, the nitrogen flow was stopped, and NH_3 was introduced until adsorption of the samples was saturated. Then, the samples were cooled to 50 °C and purged with the nitrogen to remove residual NH_3 from the surface of samples. Subsequently, the samples were heated from 50 to 700 °C at a rate of 10 °C/min for NH_3 desorption.

The IR spectrum of the pyridine-adsorbed samples was obtained in the transmission mode using a Nicolet Model 710 spectrometer (Thermo Nicolet Corporation, Madison, WI, USA). The catalyst was grounded into fine powders and pretreated at 250 °C for 2 h under evacuation, then cooled to room temperature when pyridine vapor was introduced into the oven for 24 h. The physically adsorbed pyridine was removed by evacuating for 1 h and a spectrum was subsequently recorded.

The element compositions of MMT, Sn-MMT and $\text{SO}_4^{2-}/\text{Sn-MMT}$ were measured by ICP-AES (Optima 7000DV, PerkinElmer, Waltham, MA, USA). N_2 adsorption/desorption isotherms of catalysts at 77 K were collected on a Micromeritics ASAP 2010 instrument (Micromeritics Instrument Corporation, Atlanta, GA, USA). The specific surface area was calculated using the BET method.

3.4. Procedure for the Transformation of Xylose and Xylan into Furfural

Experiments for the catalytic conversion of xylose and xylan to furfural were implemented in a hydrothermal reactor. Xylose or xylan and catalysts were mixed in a desired ratio, and 2-MTHF was added as the organic layer and water as the aqueous layer. The hydrothermal reactor was put in an oven and heated. In the reaction analyses, zero time was taken to be when the temperature reached to the desired temperature. After the reaction, the reactor was cooled quickly to room temperature

with flowing water. The aqueous phase and the organic phase were separated with a separatory funnel. All the samples were filtered with 0.22 μm syringe filter prior to analysis. Every experiment was replicated at least three times and the average of results was chosen for the analysis. The deviations were lower than 5%.

3.5. Product Analysis

Furfural yields in the water phase and organic phase were measured by high-performance liquid chromatography (HPLC) (Waters Corporation, Milford, CT, USA) with a reversed-phase C18 column and a refractive index detector after dilute with deionized water. A volume ratio of 0.1 wt % acetic acid aqueous solution to acetonitrile (85/15, *v/v*) was employed as a mobile phase with a flow rate of 1.0 mL/min.

Xylose in the water phase was determined by HPLC system (Waters 2414) equipped with a refractive index detector and a Bio-rad Aminex[®] HPX-87H (300 mm \times 7.8 mm) column. 5 mM of H₂SO₄ was employed as the eluent with a 0.5 mL/min flow rate at room temperature.

Calibration curves were established for quantitative calculation based on the following equations:

$$\text{Furfural yield (for xylose, mol\%)} = \frac{\text{moles of furfural produced}}{\text{moles of starting xylose}} \times 100 \quad (1)$$

$$\text{Xylose conversion (for xylose, mol\%)} = \frac{\text{moles of xylose reacted}}{\text{moles of starting xylose}} \times 100 \quad (2)$$

$$\text{Furfural selectivity (for xylose, mol\%)} = \frac{\text{moles of furfural produced}}{\text{moles of xylose reacted}} \times 100 \quad (3)$$

$$\text{Furfural yield (for xylan, mol\%)} = \frac{\text{moles of furfural produced}}{\text{moles of starting xylose in xylan}} \times 100 \quad (4)$$

4. Conclusions

The conversions of xylose and xylan to furfural were achieved using SO₄²⁻/Sn-MMT as a solid acid catalyst in a biphasic system (2-MTHF/NaCl-water). The results showed that SO₄²⁻/Sn-MMT contained both Brønsted acid and Lewis acid sites, and was more effective than Sn-MMT due to the intercalation of SO₄²⁻ ions. This catalyst had high catalytic activity and excellent recyclability. The substitution of water by saturated NaCl solution in aqueous phase obviously improved the furfural yield from xylose, but had a negative influence on the xylan conversion. A highest furfural yield of 79.64% was achieved from xylose at 160 °C for 120 min, and 77.35% from xylan at 160 °C for 90 min. After a few recycles, the catalytic performance decreased to a small extent and this catalyst displayed the excellent reusability. Hence, the SO₄²⁻/Sn-MMT catalyst, easily prepared, with remarkable efficiency, could have promising application for biomass conversion.

Supplementary Materials: The following are available online at www.mdpi.com/2073-4344/7/4/118/s1.

Acknowledgments: This work was supported by the grants from Program for National Natural Science Foundation of China (No. 21576103), Guangdong Natural Science Funds for Distinguished Young Scholar (No. S20120011250) and Guangzhou science and technology plan project (No. 201707010059).

Author Contributions: H.L. and J.R. conceived and designed the experiments; Q.L. performed the experiments; Q.L., L.J. and X.W. analyzed the data; C.L. and R.S. contributed reagents/materials/analysis tools; Q.L. wrote the paper.

Conflicts of Interest: The authors declare no conflict of interest.

References

1. Mardhiah, H.H.; Ong, H.C.; Masjuki, H.H.; Lim, S.; Lee, H.V. A review on latest developments and future prospects of heterogeneous catalyst in biodiesel production from non-edible oils. *Renew. Sustain. Energy Rev.* **2017**, *67*, 1225–1236. [CrossRef]

2. Guldhe, A.; Singh, P.; Ansari, F.A.; Singh, B.; Bux, F. Biodiesel synthesis from microalgal lipids using tungstated zirconia as a heterogeneous acid catalyst and its comparison with homogeneous acid and enzyme catalysts. *Fuel* **2017**, *187*, 180–188. [[CrossRef](#)]
3. Liu, S.; Amada, Y.; Tamura, M.; Nakagawa, Y.; Tomishige, K. One-pot selective conversion of furfural into 1,5-pentanediol over a Pd-added Ir–ReO_x/SiO₂ bifunctional catalyst. *Green Chem.* **2014**, *16*, 617–626. [[CrossRef](#)]
4. Agirrezabal-Telleria, I.; Hemmann, F.; Jäger, C.; Arias, P.L.; Kemnitz, E. Functionalized partially hydroxylated MgF₂ as catalysts for the dehydration of d-xylose to furfural. *J. Catal.* **2013**, *305*, 81–91. [[CrossRef](#)]
5. Shi, X.; Wu, Y.; Yi, H.; Rui, G.; Li, P.; Yang, M.; Wang, G. Selective preparation of furfural from xylose over sulfonic acid functionalized mesoporous SBA-15 materials. *Energies* **2011**, *4*, 669. [[CrossRef](#)]
6. Sádaba, I.; Ojeda, M.; Mariscal, R.; Granados, M.L. Silica-poly(styrenesulphonic acid) nanocomposites for the catalytic dehydration of xylose to furfural. *Appl. Catal. B Environ.* **2014**, *150–151*, 421–431. [[CrossRef](#)]
7. Choudhary, V.; Pinar, A.B.; Sandler, S.I.; Vlachos, D.G.; Lobo, R.F. Xylose isomerization to xylulose and its dehydration to furfural in aqueous media. *ACS Catal.* **2011**, *1*, 1724–1728. [[CrossRef](#)]
8. Takagaki, A.; Ohara, M.; Nishimura, S.; Ebitani, K. One-pot formation of furfural from xylose via isomerization and successive dehydration reactions over heterogeneous acid and base catalysts. *Chem. Lett.* **2010**, *39*, 838–840. [[CrossRef](#)]
9. Wang, W.J.; Ren, J.L.; Li, H.L.; Deng, A.J.; Sun, R.C. Direct transformation of xylan-type hemicelluloses to furfural via SnCl₄ catalysts in aqueous and biphasic systems. *Bioresour. Technol.* **2015**, *183*, 188–194. [[CrossRef](#)] [[PubMed](#)]
10. Izumi, Y.; Onaka, M. Liquid-phase organic reactions catalyzed by inorganic solid acids and bases. *J. Mol. Catal.* **1992**, *74*, 35–42. [[CrossRef](#)]
11. Wang, J.; Masui, Y.; Onaka, M. Direct allylation of α -aryl alcohols with allyltrimethylsilane catalyzed by heterogeneous tin ion-exchanged montmorillonite. *Tetrahedron Lett.* **2010**, *51*, 3300–3303. [[CrossRef](#)]
12. Li, H.L.; Ren, J.L.; Zhong, L.J.; Sun, R.C.; Liang, L. Production of furfural from xylose, water-insoluble hemicelluloses and water-soluble fraction of corn cob via a tin-loaded montmorillonite solid acid catalyst. *Bioresour. Technol.* **2015**, *176*, 242–248. [[CrossRef](#)] [[PubMed](#)]
13. Li, Y.; Zhang, X.-D.; Sun, L.; Zhang, J.; Xu, H.-P. Fatty acid methyl ester synthesis catalyzed by solid superacid catalyst SO₄²⁻/ZrO₂-TiO₂/La³⁺. *Appl. Energy* **2010**, *87*, 156–159. [[CrossRef](#)]
14. Lam, E.; Majid, E.; Leung, A.C.; Chong, J.H.; Mahmoud, K.A.; Luong, J.H. Synthesis of furfural from xylose by heterogeneous and reusable nafion catalysts. *Chemoschem* **2011**, *4*, 535–541. [[CrossRef](#)] [[PubMed](#)]
15. Mellmer, M.A.; Sener, C.; Gallo, J.M.; Luterbacher, J.S.; Alonso, D.M.; Dumesic, J.A. Solvent effects in acid-catalyzed biomass conversion reactions. *Angew. Chem.* **2014**, *53*, 11872–11875. [[CrossRef](#)] [[PubMed](#)]
16. Zhang, J.; Zhuang, J.; Lin, L.; Liu, S.; Zhang, Z. Conversion of d-xylose into furfural with mesoporous molecular sieve MCM-41 as catalyst and butanol as the extraction phase. *Biomass Bioenergy* **2012**, *39*, 73–77. [[CrossRef](#)]
17. Zhang, L.; Yu, H.; Wang, P.; Dong, H.; Peng, X. Conversion of xylan, d-xylose and lignocellulosic biomass into furfural using AlCl₃ as catalyst in ionic liquid. *Bioresour. Technol.* **2013**, *130*, 110–116. [[CrossRef](#)] [[PubMed](#)]
18. Zhang, T.; Li, W.; Xu, Z.; Liu, Q.; Ma, Q.; Jameel, H.; Chang, H.M.; Ma, L. Catalytic conversion of xylose and corn stalk into furfural over carbon solid acid catalyst in gamma-valerolactone. *Bioresour. Technol.* **2016**, *209*, 108–114. [[CrossRef](#)] [[PubMed](#)]
19. Xin, K.; Song, Y.; Dai, F.; Yu, Y.; Li, Q. Liquid–liquid equilibria for the extraction of furfural from aqueous solution using different solvents. *Fluid Phase Equilib.* **2016**, *425*, 393–401. [[CrossRef](#)]
20. Wang, J.; Masui, Y.; Onaka, M. Synthesis of α -amino nitriles from carbonyl compounds, amines, and trimethylsilyl cyanide: Comparison between catalyst-free conditions and the presence of tin ion-exchanged montmorillonite. *Eur. J. Org. Chem.* **2010**, *2010*, 1763–1771. [[CrossRef](#)]
21. Wang, J.; Ren, J.; Liu, X.; Xi, J.; Xia, Q.; Zu, Y.; Lu, G.; Wang, Y. Direct conversion of carbohydrates to 5-hydroxymethylfurfural using Sn-Mont catalyst. *Green Chem.* **2012**, *14*, 2506. [[CrossRef](#)]
22. Shinde, S.; Rode, C. Selective self-etherification of 5-(hydroxymethyl)furfural over Sn-Mont catalyst. *Catal. Commun.* **2017**, *88*, 77–80. [[CrossRef](#)]
23. Liu, D.; Yuan, P.; Liu, H.; Cai, J.; Tan, D.; He, H.; Zhu, J.; Chen, T. Quantitative characterization of the solid acidity of montmorillonite using combined FTIR and TPD based on the NH₃ adsorption system. *Appl. Clay Sci.* **2013**, *80–81*, 407–412. [[CrossRef](#)]

24. Liu, D.; Yuan, P.; Liu, H.; Cai, J.; Qin, Z.; Tan, D.; Zhou, Q.; He, H.; Zhu, J. Influence of heating on the solid acidity of montmorillonite: A combined study by DRIFT and Hammett indicators. *Appl. Clay Sci.* **2011**, *52*, 358–363. [[CrossRef](#)]
25. Reddy, C.R.; Bhat, Y.S.; Nagendrappa, G.; Jai Prakash, B.S. Brønsted and Lewis acidity of modified montmorillonite clay catalysts determined by FT-IR spectroscopy. *Catal. Today* **2009**, *141*, 157–160. [[CrossRef](#)]
26. Azzouz, A.; Nistor, D.; Miron, D.; Ursu, A.V.; Sajin, T.; Monette, F.; Niquette, P.; Hausler, R. Assessment of acid–base strength distribution of ion-exchanged montmorillonites through NH₃ and CO₂-TPD measurements. *Thermochim. Acta* **2006**, *449*, 27–34. [[CrossRef](#)]
27. Chen, W.-H.; Ko, H.-H.; Sakthivel, A.; Huang, S.-J.; Liu, S.-H.; Lo, A.-Y.; Tsai, T.-C.; Liu, S.-B. A solid-state NMR, FT-IR and TPD study on acid properties of sulfated and metal-promoted zirconia: Influence of promoter and sulfation treatment. *Catal. Today* **2006**, *116*, 111–120. [[CrossRef](#)]
28. Zhou, Y.; Niu, S.; Li, J. Activity of the carbon-based heterogeneous acid catalyst derived from bamboo in esterification of oleic acid with ethanol. *Energy Convers. Manag.* **2016**, *114*, 188–196. [[CrossRef](#)]
29. Li, H.L.; Deng, A.J.; Ren, J.L.; Liu, C.Y.; Wang, W.J.; Peng, F.; Sun, R.C. A modified biphasic system for the dehydration of D-xylose into furfural using SO₄²⁻/TiO₂-ZrO₂/La³⁺ as a solid catalyst. *Catal. Today* **2014**, *234*, 251–256. [[CrossRef](#)]
30. Lou, W.Y.; Zong, M.H.; Duan, Z.Q. Efficient production of biodiesel from high free fatty acid-containing waste oils using various carbohydrate-derived solid acid catalysts. *Bioresour. Technol.* **2008**, *99*, 8752–8758. [[CrossRef](#)] [[PubMed](#)]
31. Chheda, J.N.; Dumesic, J.A. An overview of dehydration, aldol-condensation and hydrogenation processes for production of liquid alkanes from biomass-derived carbohydrates. *Catal. Today* **2007**, *123*, 59–70. [[CrossRef](#)]
32. Deng, A.; Lin, Q.; Yan, Y.; Li, H.; Ren, J.; Liu, C.; Sun, R. A feasible process for furfural production from the pre-hydrolysis liquor of corncob via biochar catalysts in a new biphasic system. *Bioresour. Technol.* **2016**, *216*, 754–760. [[CrossRef](#)] [[PubMed](#)]
33. Roman-Leshkov, Y.; Barrett, C.J.; Liu, Z.Y.; Dumesic, J.A. Production of dimethylfuran for liquid fuels from biomass-derived carbohydrates. *Nature* **2007**, *447*, 982–985. [[CrossRef](#)] [[PubMed](#)]
34. Guenic, S.L.; Delbecq, F.; Ceballos, C.; Len, C. Microwave-assisted dehydration of d-xylose into furfural by diluted inexpensive inorganic salts solution in a biphasic system. *J. Mol. Catal. A Chem.* **2015**, *410*, 1–7. [[CrossRef](#)]
35. Dias, A.S.; Lima, S.; Carriazo, D.; Rives, V.; Pillinger, M.; Valente, A.A. Exfoliated titanate, niobate and titanoniobate nanosheets as solid acid catalysts for the liquid-phase dehydration of d-xylose into furfural. *J. Catal.* **2006**, *244*, 230–237. [[CrossRef](#)]
36. Xing, R.; Qi, W.; Huber, G.W. Production of furfural and carboxylic acids from waste aqueous hemicellulose solutions from the pulp and paper and cellulosic ethanol industries. *Energy Environ. Sci.* **2011**, *4*, 2193–2205. [[CrossRef](#)]
37. Zhang, T.; Kumar, R.; Wyman, C.E. Enhanced yields of furfural and other products by simultaneous solvent extraction during thermochemical treatment of cellulosic biomass. *RSC Adv.* **2013**, *3*, 9809. [[CrossRef](#)]
38. Binder, J.B.; Blank, J.J.; Cefali, A.V.; Raines, R.T. Synthesis of furfural from xylose and xylan. *ChemSusChem* **2010**, *3*, 1268–1272. [[CrossRef](#)] [[PubMed](#)]
39. Lessard, J.; Morin, J.-F.; Wehrung, J.-F.; Magnin, D.; Chornet, E. High yield conversion of residual pentoses into furfural via zeolite catalysis and catalytic hydrogenation of furfural to 2-methylfuran. *Top. Catal.* **2010**, *53*, 1231–1234. [[CrossRef](#)]
40. Agirrezabal-Telleria, I.; Requies, J.; Güemez, M.B.; Arias, P.L. Dehydration of d-xylose to furfural using selective and hydrothermally stable arenesulfonic SBA-15 catalysts. *Appl. Catal. B Environ.* **2014**, *145*, 34–42. [[CrossRef](#)]
41. Bhaumik, P.; Dhepe, P.L. Exceptionally high yields of furfural from assorted raw biomass over solid acids. *RSC Adv.* **2014**, *4*, 26215. [[CrossRef](#)]
42. Dias, A.S.; Pillinger, M.; Valente, A.A. Dehydration of xylose into furfural over micro-mesoporous sulfonic acid catalysts. *J. Catal.* **2005**, *229*, 414–423. [[CrossRef](#)]
43. Dias, A.S.; Lima, S.; Pillinger, M.; Valente, A.A. Modified versions of sulfated zirconia as catalysts for the conversion of xylose to furfural. *Catal. Lett.* **2007**, *114*, 151–160. [[CrossRef](#)]

44. Lima, S.; Pillinger, M.; Valente, A.A. Dehydration of d-xylose into furfural catalysed by solid acids derived from the layered zeolite Nu-6(1). *Catal. Commun.* **2008**, *9*, 2144–2148. [[CrossRef](#)]
45. Li, H.; Chen, X.; Ren, J.; Deng, H.; Peng, F.; Sun, R. Functional relationship of furfural yields and the hemicellulose-derived sugars in the hydrolysates from corncob by microwave-assisted hydrothermal pretreatment. *Biotechnol. Biofuels* **2015**, *8*, 127. [[CrossRef](#)] [[PubMed](#)]



© 2017 by the authors. Licensee MDPI, Basel, Switzerland. This article is an open access article distributed under the terms and conditions of the Creative Commons Attribution (CC BY) license (<http://creativecommons.org/licenses/by/4.0/>).